Sex differences in estimated brain metabolism in relation to body growth through adolescence

Simon N Vandekar[1], Haochang Shou[1],
Theodore D Satterthwaite[2], Russell T Shinohara[1],
Alison K Merikangas[2], David R Roalf[2], Kosha Ruparel[2],
Adon Rosen[2], Efstathios D Gennatas[2], Mark A Elliott[3],
Christos Davatzikos[3], Ruben C Gur[2,3,4,5], Raquel E Gur[2,3,5]
and John A Detre[3,5]

Abstract
The human brain consumes a disproportionate amount of the body's overall metabolic resources, and evidence suggests that brain and body may compete for substrate during development. Using perfusion MRI from a large cross-sectional cohort, we examined developmental changes of MRI-derived estimates of brain metabolism, in relation to weight change. Nonlinear models demonstrated that, in childhood, changes in body weight were inversely related to developmental age-related changes in brain metabolism. This inverse relationship persisted through early adolescence, after which body and brain metabolism began to decline. Females achieved maximum body growth approximately two years earlier than males, with a correspondingly earlier stabilization of brain metabolism to adult levels. These findings confirm prior findings with positron emission tomography performed in a much smaller cohort, demonstrate that relative brain metabolism can be inferred from noninvasive MRI data, and extend observations on the associations between body growth and brain metabolism to sex differences through adolescence.

Introduction

The mammalian brain is a metabolically demanding organ that is estimated to require 6 kCal per billion neurons per day.[1] The adult human brain represents only ~2% of body weight, yet it consumes approximately 20% of total body metabolic substrate.[2] As such, the caloric intake needed to supply the brain's metabolic requirement has been considered an evolutionary constraint on brain size.[3] While most vertebrate species use less than 10% of their basal metabolism to support brain function in adulthood, primates and particularly humans use considerably more.[4]

Brain energy requirements are even larger in childhood.[5] Some evidence suggests that brain and body development may be in competition for metabolic substrate and the considerable metabolic needs of the

[1]Department of Biostatistics, Epidemiology, and Informatics, University of Pennsylvania, Philadelphia, PA, USA
[2]Department of Psychiatry, University of Pennsylvania, Philadelphia, PA, USA
[3]Department of Radiology, University of Pennsylvania, Philadelphia, PA, USA
[4]Philadelphia Veterans Administration Medical Center, Philadelphia, PA, USA
[5]Department of Neurology, University of Pennsylvania, Philadelphia, PA, USA

The first two authors share co-first authorship.

Corresponding author:
John A Detre, Department of Neurology, Perelman School of Medicine, University of Pennsylvania, 3W Gates Pavilion, 3400 Spruce Street Philadelphia, PA 19104, USA.
Email: detre@mail.med.upenn.edu

developing brain may account for the remarkably slow early development of the human body relative to other species.[2,5,6] Kuzawa et al.[6] combined positron emission tomography (PET) data on brain metabolic rates in childhood[7] with information about body growth rates and metabolism to demonstrate that brain glucose utilization, relative to total body metabolism, does not peak in infancy, when brain mass is highest relative to body mass. Rather, it occurs during childhood when body growth rates are slowest and synaptic proliferation is maximal.[8] Their findings support the notion of brain and body competition for metabolic substrate, but were limited by a small sample size with only three measures of adolescent brain metabolism after age 10 and no information about sex differences.

The most rapid phase of human body growth occurs during adolescence,[9] when brain development is associated with continued thinning of cortex due to white matter expansion[10–16] and reorganization of prefrontal synaptic connections.[17,18] Notably, the adolescent growth spurt is unique to humans.[19] Adolescence is also associated with the emergence of highly significant sex differences in body growth, with females reaching full body mass index (BMI) considerably earlier than males.[20] Thus, it is of interest to further understand the relationship between brain and body metabolism during this period of development.

Here, we evaluated sex differences in brain metabolism as it relates to body growth in the Philadelphia Neurodevelopmental Cohort (PNC), a large population-based sample of over 9500 individuals aged 8–21 years from the greater Philadelphia area. Imaging data were collected in a subset of 1600 subjects, and included quantitative magnetic resonance imaging of cerebral blood flow (CBF) using arterial spin labeled (ASL) perfusion magnetic resonance imaging (MRI).[21,22] We previously reported age-related differences in CBF in 921 PNC participants, demonstrating a progressive reduction in gray matter CBF from age 8 through 18 and a more subtle increase in CBF in early adulthood.[23] Significant sex differences in CBF developmental changes were also observed, with females demonstrating an increase in CBF in late adolescence, while CBF continued to decline in males.

CBF is thought to be tightly coupled to neural activity,[24] and hence serves as a proxy for regional brain metabolism that can be acquired entirely noninvasively. In contrast to PET scanning, ASL MRI is totally noninvasive and does not require exposure to ionizing radiation. To relate our developmental data to the PET measurements of brain glucose metabolism,[6] we used CBF, demographic variables including self-reported weight, and published values relating glucose metabolism to CBF[6,25,26] to estimate the percentage of resting metabolic rate attributable to the brain (%RMR).

We derived the development-related changes for mean CBF, whole brain glucose consumption, and %RMR as it relates to body growth through adolescence. We also included regional investigations of these measures of brain metabolism in precuneus and superior frontal gyrus (SFG), which have been identified as early and late developing CBF trajectories, respectively, in developmental reports.[27] Finally, we used these MRI-derived measures to investigate sex differences in the relationship between body growth rate and brain metabolism.

Methods

The study procedures were performed according to the ethical guidelines set forth in the Belmont Report and approved by the Institutional Review Boards at University of Pennsylvania (Penn) and Children's Hospital of Philadelphia (CHOP). All subjects or their parent or legal guardian gave informed consent and minors gave assent. The Institutional Review Boards at Penn and CHOP both approved study procedures.

Sample description

Two cross-sectional subsamples of the PNC were used to estimate weight-change and imaging derived measures separately (Table 1). Self- or collateral informant-reported weight and CBF derived measures were analyzed in two subsets of the PNC. The weight data quality assurance (QA) was performed using the SAS program provided by the Center for Disease Control (CDC; www.cdc.gov/nccdphp/dnpao/growthcharts/resources/sas.htm). From a total sample of 9498, 1970 did not have weight data. An additional 46 were flagged as biologically implausible using the CDC program based on age and sex standardized weight z-scores below −5 or above 8. Weight and weight-change curves were estimated from the remaining sample of 7482 whose data passed the QA procedure. The subset used includes 915 subjects that are family members (e.g. siblings, cousins). Imaging data were collected in a subset of 1601 subjects. Clinical and imaging

Table 1. Sample demographics for weight-change and imaging data curve estimation.

	n	Female	White	Black	Other	Mean age (SD)
Self-reported weight	7482	3851	4317	2298	867	13.73 (3.51)
Imaging	1098	609	467	503	128	14.4 (3.43)

Note: Age is mean (standard deviation).

exclusionary criteria yielded a total of 1098 subjects for estimation of CBF age trajectories.[23] Clinical exclusionary criteria included a history of medical disorders that affect the brain, a history of inpatient psychiatric hospitalization, or current use of a psychotropic medication. Imaging exclusionary criteria included missing data, excessive motion (mean relative displacement >0.5 mm), low temporal signal-to-noise ratio (tSNR < 30) in raw time series data, poor image coverage, or an excessive number of voxels that had ceiling intensity values at some point in the time series (>500).[23] Of the 1601 subjects imaged as part of the PNC, 23 did not have CBF imaging data collected. An additional 181 were excluded as part of the CBF data imaging QA,[23] which included excluding subjects with any negative values in the regions of interest (ROIs). Finally, 299 were excluded based on the clinical criteria. A subsample of 824 subjects who had self-reported weight and imaging data were used to estimate the percentage of resting metabolic rate attributable to the brain (%RMR; see methods below).

Image acquisition, QA, and preprocessing

All imaging data were acquired on the same scanner as part of the same imaging protocol as previously described.[22,23] CBF was imaged using a custom pseudo-continuous arterial spin labeling (pCASL) sequence.[28] The sequence used a single-shot spin-echo echo-planar imaging readout. The arterial spin labeling parameters were TR 4 s, TE 15 ms, flip angle 90/180°, FOV 220 × 220 mm, matrix 96 × 96 × 20, slice thickness/gap 5/1 mm, effective voxel resolution 2.3 × 2.3 × 6 mm, label duration 1500 ms, postlabel delay 1,200 ms, GRAPPA 2, 80 volumes (40 label, 40 control). Before the pCASL sequence, a magnetization-prepared, rapid acquisition gradient-echo T1-weighted image was acquired for use in spatial normalization to standard atlas space, using the following parameters: TR 1,810 ms, TE 3.51 ms, TI 1,100 ms, FOV 180 × 240 mm, matrix 192 × 256, 160 slices, slice thickness/gap 1 mm/0 mm, flip angle 9°, GRAPPA 2, effective voxel resolution of 0.9 × 0.9 × 1 mm, and total acquisition time 3:28 min. Additionally, a B0 field map was acquired for application of distortion correction procedures, using a double-echo gradient recall echo sequence: TR 1,000 ms, TE1 2.69 ms, TE2 5.27 ms, 44 slices, slice thickness/gap 4 mm/0 mm, flip angle 60°, FOV = 240 mm, effective voxel resolution of 3.8 × 3.8 × 4 mm.

All imaging data were loaded into an XNAT database that included custom front-end (QLUX) software that monitored QA by checking that acquisition parameters matched a study-defined template. ASL data were pre-processed using standard tools included with FSL.[29] Following distortion correction using the B0

map with FUGUE, the first four image pairs were removed, the time series was realigned with MCFLIRT,[30] the skull was removed with BET,[31] and the image was smoothed at 6 mm FWHM using SUSAN.[32] CBF was quantified from control-label pairs using ASL Toolbox.[33] As described previously,[23] the T1 relaxation parameter was modeled on an age- and sex-specific basis.[34] This model accounts for the fact that T1 relaxation time differs according to age and sex, and has been shown to enhance the accuracy and reliability of results in developmental samples.[35] The procedure is discussed in detail in the Supplement of our previous report.[23] The T1 image was co-registered to the CBF image using boundary-based registration,[36] and CBF values were averaged within each anatomically defined parcel.

T1-weighted structural images were processed using tools included in ANTs.[37] Brain extraction was guided using a study-specific set of tissue priors; bias-field correction used N4.[38] In order to parcellate the brain into anatomically-defined regions, we used an advanced multi-atlas labeling approach[39]. Specifically, 24 young adult T1 images from the OASIS data set that were manually labeled by Neuromorphometrics, Inc. (http://Neuromorphometrics.com/) were registered to each subject's T1 image using the top-performing top-performing SyN diffeomorphic registration.[40,41] These label sets were synthesized into a final parcellation using joint label fusion.[42] The labeled images allowed estimation of regional and whole brain volumes. The T1 image was co-registered to the CBF image using boundary-based registration,[36] and CBF values were averaged within each anatomically defined parcel.

Brain glucose consumption and %RMR estimation

Brain glucose metabolism (CMRGlc) and brain metabolism as a percentage of total resting metabolic rate of the body (%RMR) were estimated for the whole brain and anatomically defined parcels using the MRI-derived CBF maps and a CMRGlc:CBF ratio derived from the literature. Brain metabolism was estimated in the units of grams of glucose consumed per day based on CBF quantified with ASL using the formula

$$(grams\ glucose)/day = CBF \times Volume \times Density$$
$$\times \frac{grams\ glucose}{ml\ blood}$$

where $(grams\ glucose)/day$ denotes the grams of glucose consumed per day.

- *CBF* was whole brain or regional mean CBF in *ml/grams/day* obtained by summing MRI-derived measurements of CBF in ml/100 g/min over voxels

in either whole brain or a region of interest, dividing by 100 (to convert 100 grams to grams), and multiplying by the number of minutes in 24 h (1440).

- *Volume* was the subject's whole brain or regional volume in milliliters obtained from the segmentation of the T1-structural MRI.
- *Density* was mean brain density ($1.081 \times grams/ml$) obtained from a previous study using ex vivo tissue samples of males and females ages 17–84[2,6] and was assumed to be constant across age, sex, brain region, and development.
- Estimation of glucose metabolism from CBF also assumed that the rate of grams of glucose consumption per milliliter of CBF $\left(\frac{grams\ glucose}{ml\ blood}\right)$ was constant across sex, brain region, and development and was equal to

$$(grams\ glucose)/(ml\ blood)$$
$$= 0.33\left(\frac{\mu mol}{cm^3 \times min}\right)/0.43\left(\frac{ml}{cm^3 \times min}\right)$$
$$\times 180.16 \times 10^{-6}\frac{grams}{\mu mol}$$

The rate of average glucose uptake $0.33\left(\frac{\mu mol}{cm^3 \times min}\right)$ and the rate of CBF $0.43\left(\frac{ml}{cm^3 \times min}\right)$ were obtained from a recent PET study.[25] Whole-body resting metabolic rate (RMR) was estimated in grams of glucose from self-reported weight, age, and sex using previously published formulas. To achieve this, piecewise linear functions[43] were first used to compute RMR in kilocalories then these values were converted to grams of glucose by dividing by $3.72\ kcal/(gram\ glucose)$.[44] The formulas to compute RMR are given in the supplement. %RMR is estimated by dividing brain glucose consumption by RMR. We provide the code used to compute these values and to perform analyses in this manuscript online at https://bitbucket.org/simonvandekar/brain-body.

Body weight and imaging outcome model fitting

Our main focus was to characterize sex differences in the age-dependent bivariate relationship between body growth and brain metabolism. Body growth and brain metabolism were estimated using weight-change and %RMR, respectively. First, the population weight curve was estimated and then the weight-change curve was obtained by differentiating the weight curve with respect to age. As we were utilizing a cross-sectional sample where the rate of weight-change was not directly observed for each subject, the estimation was restricted to the marginal relationships of weight-change with age, and of %RMR with age separately. The curves were estimated and tested

for each variable and plotted together to investigate their relationship.

All the statistical analyses were implemented in R 3.3.1.[45] The software package 'mgcv' 1.12[46,47] was used to conduct spline-based model fitting. The imaging outcome measures and body weight were modeled as nonlinear functions of age using generalized additive models (GAMs). Nonlinear functions for each sex were fit using a 12 knot P-spline bases with a third degree penalty in order to ensure flexibility of the weight-change trajectories after differentiation. A single smoothing parameter, estimated by restricted maximum likelihood (REML), was used for male and female age curves. After obtaining the estimated developmental weight curves, the population-level weight-change curve was differentiated with respect to age by taking small finite differences ($\Delta = 0.0001$) from the functions that define the spline basis. Race was included as a covariate in the body-weight model, and race, in-scanner motion, and regional gray matter density were included as covariates in CBF models. Confidence intervals for the fitted curves were estimated using 2000 simulations. Confidence intervals for age bubbles in the bivariate body growth and brain metabolism plots (Figure 3) were estimated from the standard errors using a normal approximation.

Testing hypotheses of nonlinear functions

For each outcome (weight-change or imaging measure), we conducted tests for nonlinear sex difference in the weight-change curves (i.e. the sex by age interaction). For the weight-change curve, the test is equivalent to testing for a nonlinear age by sex interaction on weight over a linear age by sex interaction. This is because the derivative of a line is a constant; if the difference in weight curves between males and females was linear or constant then the difference in the weigh-change curves would be constant or zero. Thus, for weight, only coefficients for higher order spline terms were tested. Specifically, to test the interaction for weight, we fit the following two models and performed F-test for the difference

$$W_i = f(age_i) + \beta_2 sex_i + \beta_3 age_i \times sex_i + covariates$$
$$W_i = f_M(age_i) + f_F(age_i) + \gamma_1 sex_i + covariates$$

where W_i was the observed self-reported weight, $f(age_i)$ was a nonlinear function of age for both sexes and the β parameters encoded the linear difference in age between males and females. $f_M(age_i)$ and $f_F(age_i)$ are nonlinear functions of age for males and females, respectively. The test for the difference between these models had 10 degrees of freedom. We performed hypothesis tests using unpenalized splines in order to maintain an

accurate type 1 error rate[47] and used Holm's procedure across ROIs to compute adjusted *p*-values.

To investigate whether %RMR and CBF in the precuneus or SFG reached maturity earlier, we compared the first age after 10 when the slope of the developmental curve was zero. In order to test the difference between the age that the slope of the curve reached zero in SFG and precuneus, we used 1000 bootstrap samples to estimate the distribution of the difference and computed the probability that the difference was less than zero (see Supplement for details).

Results

Nonlinear weight-change developmental curves differ in males and females

To understand the developmental course of body weight-change, nonlinear weight-change curves were estimated and differentiated to obtain the estimated weight-change curve. The estimated growth curves produced by this procedure closely match the shape of the median estimates reported by the Center for Disease Control[48] (Figure 1(a) and (b)), indicating the reliability of the sample data and model fit. Results from hypothesis testing suggested that the rates of weight-change estimated from self-reported weight are not constant over time for males ($F = 15.74$, df1 = 10, df2 = 7454, $p < 0.001$) or for females ($F = 27.00$, df1 = 10, df2 = 7454, $p < 0.001$). In addition, we were able to detect a sex difference in developmental weight-change curves ($F = 3.90$, df1 = 10, df2 = 7456, $p < 0.001$). Weight-change curves demonstrate an earlier peak for females (age = 11) than males (age = 13; Figure 1(c)). The confidence interval for male weight-change covered zero at age 19 (Figure 1(c)), indicating no significant growth after that age for males. For females, weight-change covered zero between 17 and 18, but increased slightly afterward (Figure 1(c)). Between ages 13 to 18, female weight-change was
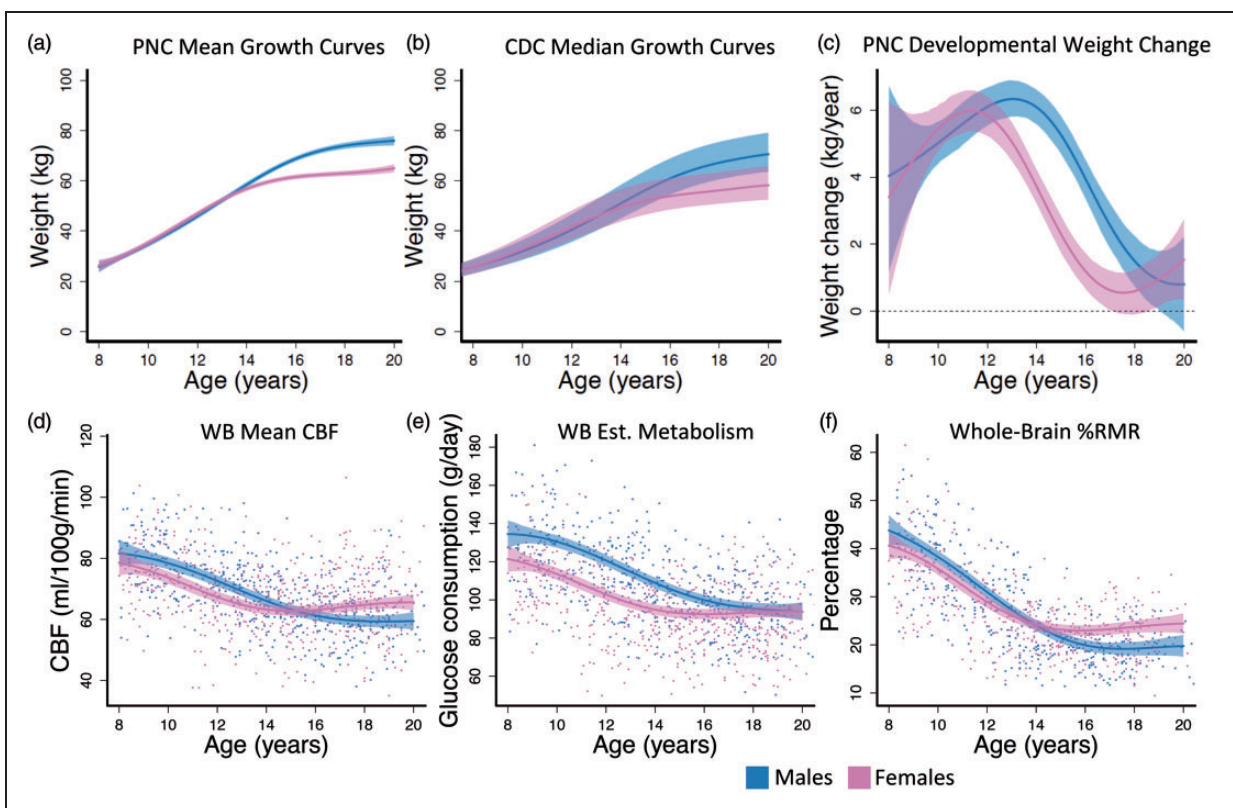

Figure 1. Males and females exhibited different developmental curves in weight, weight-change, and whole-brain CBF-derived imaging measures. (a) PNC estimated mean growth curves. (b) CDC median weight trajectories from May 2000. Dashed lines are 25% and 75% percentiles. (c) Females had an earlier peak and decline in rate of weight-change than males. (d) CBF declined for females until age 15 where it began to increase, while CBF in males declined until age 18 where the curve flattens. (e) Whole-brain glucose consumption was lower in females through development until adulthood where males and females had identical brain glucose consumption. (f) %RMR was approximately equal in males and females until reaching adult resting levels. Fitted curves are estimated with generalized additive models (GAMs). Colored dashed lines in (a) and (c–f) are 95% simultaneous confidence intervals; WB: whole brain; Est: estimated.

significantly slower than males. Together, this suggests that the female weight-change curve appears shifted approximately two years earlier than males.

CBF and %RMR development-related changes

To assess development-related changes of brain metabolism, total brain glucose and %RMR were estimated from regional CBF data and demographic variables using published formulas[6,25,26,43] and as described in the Methods. Changes in CBF, brain glucose, and %RMR were then modeled as nonlinear functions of age for each sex. Significant sex differences in age-related changes of CBF, brain glucose, and %RMR were observed (Table 2; Figure 1(d) to (f)). The CBF data (Figure 1(d)) had the largest effect size (partial R^2) for the sex difference (Table 2); however, all three outcome measures declined in early adolescence and were lower in females. From ages 15–20, CBF in females increased slightly, plateauing at higher adult levels than males. Female %RMR plateaued at approximately age 15, whereas male %RMR continued to decline until age 18, similar to the ages where female CBF began to increase and male CBF began to level off. In contrast, whole-brain estimated glucose consumption ultimately reached similar levels in males and females (Figure 1(e)). Females had higher CBF and %RMR than males in late adolescence and young adulthood. Sex differences in %RMR prior to age 14 were less pronounced relative to those seen in CBF (Figure 1(f)).

The age curves of whole-brain glucose consumption estimated using ASL-derived CBF were approximately 20% lower than those obtained using PET by Kuzawa et al.[6] These differences were consistent across sexes (Table S1), but by age 20, MRI-derived values closely matched PET-derived levels in males. MRI-derived %RMR showed a similar relationship to PET-derived %RMR, and the %RMR plateau at age 20 in males and females closely matched adult levels in Kuzawa et al.[6] (Table S2).

We selected precuneus and SFG as representative posterior and frontal regions to probe differences in early and late developing structures.[27] Both precuneus and SFG showed significant sex differences in CBF, regional glucose consumption, and %RMR age-related changes (Table 3; Figure 2). The effect sizes were comparable across measures, but were slightly higher for the precuneus. To investigate the age when CBF and %RMR reached adult levels, we used the fitted curves to estimate the first age after 10 when the slope of the developmental curve was zero, indicating that the measure stopped changing. Our results are consistent with previous findings,[27] with the CBF curve in SFG reaching adult levels slightly later than precuneus; however,

Table 2. Hypothesis tests for sex differences in development-related changes of whole-brain CBF, brain glucose consumption, and the percentage of resting metabolic rate attributable to the brain (%RMR).

	df1	df2	F-value	p-value	Partial R^2
CBF	11	1070	5.7	<0.001	0.04
Brain glucose	11	1070	4.2	<0.001	0.03
%RMR	11	802	4.9	<0.001	0.03

Note: df1 and df2 indicate numerator and denominator degrees of freedom for the F-statistic. p-values are Holm adjusted. %RMR percentage of resting metabolic rate; CBF: cerebral blood flow.

Table 3. Regional hypothesis tests for sex differences in development-related changes of CBF, brain glucose consumption, and the percentage of resting metabolic rate attributable to the brain (%RMR).

	df1	df2	F-value	p-value	Partial R^2
Precuneus					
CBF	11	1070	4.1	<0.001	0.03
Brain glucose	11	1070	3.0	0.001	0.02
%RMR	11	802	4.3	<0.001	0.02
SFG					
CBF	11	1070	4.7	<0.001	0.04
Brain glucose	11	1070	4.0	<0.001	0.03
%RMR	11	802	5.0	<0.001	0.03

Note: Precuneus and superior frontal gyrus (SFG) were selected as representatives of early and late developing regions, respectively. p-values are Holm adjusted. %RMR percentage of resting metabolic rate; SFG: superior frontal gyrus; CBF: cerebral blood flow.

the difference was not significant in CBF or %RMR (see supplement for further discussion).

Joint weight-change and CBF curves differ in males and females

To assess the evidence supporting brain metabolism and body growth competition, we constructed 95% confidence regions for each age level using the weight-change and %RMR curves shown in Figures 1 and 2. Whole-brain bivariate curves corroborated and extended previous findings for both sexes[6] (Figure 3). Specifically, in males, there was a negative association between %RMR and weight-change prior to peak weight-change at age 13 as indicated by a modest negative slope between age bubbles in ages less than 13 (Figure 3(a)). Similarly, for females there was also a negative slope between age bubbles prior to peak weight-change, which occurred at approximately age 11 (Figure 3(b)). At younger ages, female bivariate
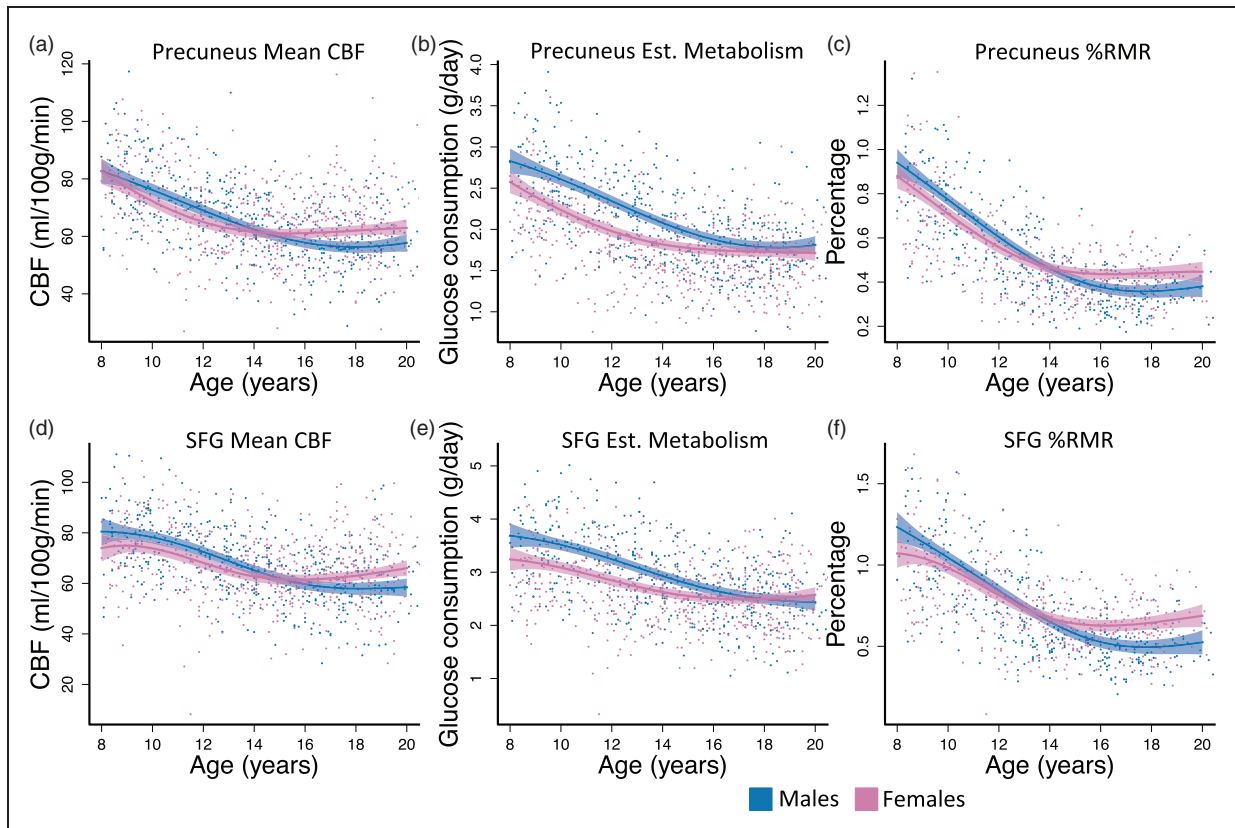
Figure 2. Development-related changes in brain for two select structural ROIs. (a, d) CBF reached adult levels at approximately the same time in precuneus and SFG; however, SFG had a later peak CBF in childhood at approximately age 8 or 9. The peak for precuneus was not detectable in this age range. (b, e) Regional glucose consumption declined in both regions until reaching approximately the same level in adulthood for males and females. (c, f) %RMR decreases in both sexes for both regions. Female's curves leveled at a higher resting value by age 15. Fitted curves are estimated with generalized additive models (GAMs). Dashed lines are 95% simultaneous confidence intervals; Est: estimated.

curves appeared to be shifted forward temporally relative to males by approximately one to two years. For example, the mean for 11-year-old females is at approximately the same position as the mean of 12-year-old males on the whole-brain bivariate plots (Figure 3(a) and (d)).

While an inverse relationship between brain metabolism and weight-changes was not present after childhood (Figure 3), observed sex differences in body growth rates did appear to be reflected in brain metabolism trajectories. Around age 14, when female growth rate was clearly declining (Figure 1(c)) and body weight was stabilizing (Figure 1(a)), female brain glucose consumption (Figure 1(e)) and %RMR (Figure 1(f)) stabilized near adult levels. The onsets of these changes were shifted to around age 16 in males.

Discussion

We used estimated brain metabolism in a large developmental cohort to examine sex differences in the relationship between brain and body metabolism. Using the CBF-derived estimates of %RMR obtained noninvasively with MRI, we found evidence to support the hypothesis that brain and body growth are inversely related in childhood and further demonstrated that this inverse relationship occurs only prior to peak weight-change. After that, %RMR and body growth rates decline together. Furthermore, this developmental shift occurs significantly earlier in females than in males, and is associated with sex differences in the transition from declining to plateau values of %RMR.

Developmental curves of brain glucose consumption and %RMR derived from ASL MRI data matched previously published results based on PET data.[6,7] MRI-derived glucose consumption and %RMR values in childhood and early adolescence were approximately 20% lower than PET-derived values, while the two measures were in much closer agreement for adults. MRI-derived estimates of %RMR reached adult levels by age 15–17, which is consistent with previous PET reports measuring brain glucose metabolism
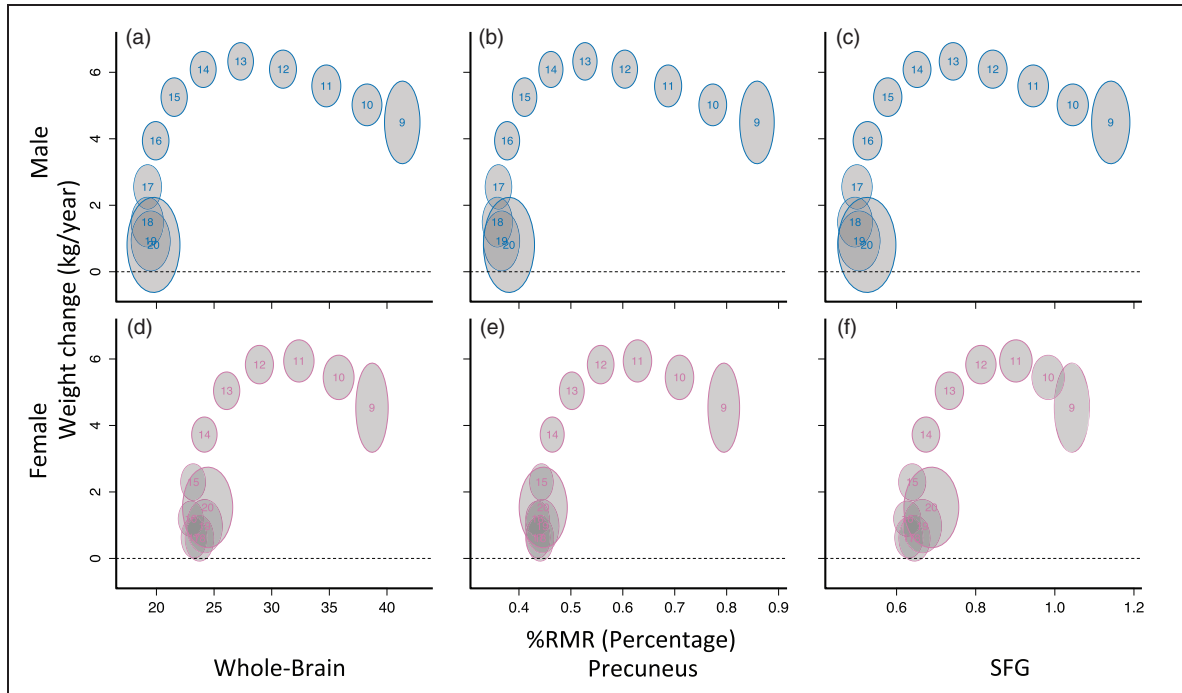
Figure 3. Whole-brain (a, d) and regional (b, c, e, f) %RMR weight-change curves differ by sex. Each curve was fit separately as a function of age using generalized additive models (GAMs), and the location for each age was plotted. Each number on the plots indicates a corresponding age; gray bubbles are 95% marginal confidence regions. Larger bubbles are due to noisier estimates toward the edges of the sample range. The bivariate relationship between weight-change and whole-brain %RMR appeared shifted forward temporally for females relative to males; however, after peak weight change, female %RMR was higher in all regions. %RMR reaches adult levels before weight-change reaches zero.

directly.[7] Importantly, CBF-based brain glucose consumption and %RMR derived from ASL MRI are completely noninvasive, and readily obtained in large cohorts. In contrast, due to the paucity of more costly and invasive PET measures of brain glucose consumption during development, the approach of Kuzawa et al.[6] only allowed for estimation of %RMR at discrete ages across subjects, after combining PET and MRI data from separate cohorts. Because the MRI-derived %RMR data provided a within-subject measure of relative brain energy consumption (i.e. both CBF and body weight were derived from the same subject), it is possible that the MRI-derived %RMR estimates obtained in this study are more accurate than prior estimates, despite not measuring glucose metabolism directly. The concordance between CBF- and PET-based measures of brain metabolism across development also provides additional support for the notion that CBF and metabolism are closely coupled in the brain.

Postnatal human brain development can be characterized by an initial phase of synaptic proliferation followed by a subsequent phase of synaptic pruning and the myelination of brain networks. This process begins with sensorimotor networks in childhood and concludes with higher order association cortex, most notably the prefrontal cortex in young adulthood. Brain energy utilization was initially thought to primarily support synaptic activity,[49] and consistent with this, human brain metabolism is maximal at approximately age 5 in childhood[6] when rapid brain growth and particularly synaptogenesis are occurring. The younger ages of our sample likely capture the end of this earlier developmental stage, which is characterized by a reduction in %RMR and increasing body weight-change. Sex differences in the %RMR and weight-change relationship at younger ages are due to an earlier peak body-growth in females.

While the onset of adolescence is characterized by hormonally mediated changes in the body, the end of adolescence primarily reflects changes in cognitive functions associated with identity, motivation, goals, and social interactions related to transition to adulthood.[50] After peak weight-change, both female and male %RMR were observed to decline and then asymptote to approach adult values. This transition occurs approximately two years earlier in females than in males, and %RMR values in females also appear to increase slightly after body growth rates reach zero. This late increase in relative brain metabolism may

reflect neuroplastic changes associated with cognitive skill development that largely follows the development of adult physical traits in adolescence. While most of brain energy utilization has been attributed to synaptic activity, more recent estimates suggest that non-signaling processes represent a larger fraction of total brain energy consumption than was previously thought.[51] The elimination and reorganization of pre-frontal synaptic connections[17] and the maturation of frontal networks involved in cognitive control that occurs in adolescence is likely also energetically demanding. A similar increase may occur in males, but is not captured in the age range of these data, since male body growth rates reach zero later.

In addition to evaluating mean CBF, estimated glucose consumption, and estimated %RMR in whole brain, we also measured these values in selected ROI to assess for regional variations. Based on prior work examining the developmental trajectory of CBF,[27] we selected precuneus, which showed an early CBF peak, and SFG, which showed a later CBF peak in that study. We observed subtle differences in the developmental trajectories of mean CBF and %RMR between precuneus and SFG, but these differences were not statistically significant. However, sex differences between these trajectories remained significant in each ROI. Accordingly, the observed sex differences in developmental trajectories of whole brain CBF and %RMR probably do not simply reflect effects of underlying regional differences in global brain metabolism.

While the observed developmental changes in regional brain function roughly parallel previously documented sex differences in brain volume changes observed in a large longitudinal cohort, wherein females reached peak cerebral volume at age 10.5 and males at age 14.5,[13] the approximately three year delay between peak cerebral volume and %RMR stabilization suggests that the observed changes in brain metabolism also do not simply reflect sex differences in underlying brain structure. Furthermore, we observed corresponding sex differences in the CBF curves while controlling for underlying brain structure by including regional gray matter density as a covariate.

There are several limitations of this study that should be noted. Firstly, a fundamental assumption of our method is that the ratio of brain glucose metabolism to CBF is roughly constant across sex, brain regions, and development in healthy subjects. This assumption reflects the widely held notion that CBF and glucose metabolism are normally coupled.[52] The constant ratio between glucose metabolism and CBF we used was derived from a recent PET study in adult males, but is comparable to the ratio that can be computed from values in an earlier source in males and females.[53] As noted above, the values we obtained for

estimated brain glucose metabolism are consistent with published values based on FDG-PET data. While further validation of MRI-derived estimates of brain glucose metabolism against FDG-PET in the same subjects would be highly desirable, there are challenges in exposing healthy children and developing adolescents to ionizing radiation. This type of validation would be more realistic in healthy adults and can be obtained with concurrent ASL MRI and FDG-PET.[54] Note, that in estimating brain glucose metabolism from CBF, we also assume that brain density is constant across age, sex, brain regions, and development. Secondly, the cross-sectional nature of our analyses limits our ability to make strong conclusions about individual trajectories. Our fitted weight-change and CBF age curves may be descriptive only of the population curves. Furthermore, the use of cross-sectional data also did not allow us to statistically investigate associations between %RMR, weight-change, and cognitive measures available within the PNC neuroimaging cohort, though developmental sex differences in cognition were observed in the much larger overall PNC cohort.[55] Longitudinal data in which individual differences in weight-change, %RMR, and cognitive performance could be assessed would be required to better establish whether these individual trajectories are related.[50] Further, there are opportunities to improve the accuracy of CBF measured using ASL MRI, including improved acquisition schemes and improved modeling of CBF based on ASL MRI data.[56]

Our results support the hypothesis that brain and body growth compete for resources during childhood development and further suggest that a diverging temporal sequence of body growth between males and females in adolescence is associated with sex differences in the trajectories of brain metabolism as well. The notion that brain and body compete for metabolic resources during development has implications for human health. While it may be tempting to speculate that sufficient caloric intake could eliminate brain and body competition for substrate, obesity has been shown to blunt cerebral insulin suppression,[57] a key mechanism by which metabolic substrate is diverted from the body to the brain. Existing data also suggest that childhood obesity is associated with impairments in cognitive function[58] as well as reductions in gray matter volumes.[59] Elevated BMI in childhood is also associated with earlier pubertal changes, particularly in females,[60] and could alter the normal trajectory of functional development in the adolescent brain, potentially resulting in suboptimal maturation of cognitive circuits. While changes in brain and body metabolism appear to be linked throughout development, metabolic competition is likely complex as the brain is responsible for the allocation and intake of resources that may contribute

to changes in body growth and nutrient intake.[61] Our findings documented sex differences in these processes through critical stages in human development.

Declaration of conflicting interests

The author(s) declared no potential conflicts of interest with respect to the research, authorship, and/or publication of this article. REG served on the Advisory Board Member for Otsuka Pharmaceuticals.

Authors' contributions

Concept and design: JAD, REG, RCG, TDS, DRR, MAE. Acquisition of data: REG, RCG, CD, KR, MAE. Analysis and/or interpretation of data: SNV, HS, JAD, RTS, TDS, DRR, AKM, CD, AR, EDG. Drafting and/or revising the manuscript: JAD, SNV, HS, RTS, TDS, REG, RCG, AKM, DRR, KR, EDG, AR, MAE, CD.

Supplementary material

Supplementary material for this paper can be found at the journal website: http://journals.sagepub.com/home/jcb

References

1. Herculano-Houzel S. Scaling of brain metabolism with a fixed energy budget per neuron: implications for neuronal activity, plasticity and evolution. *PLoS One* 2011; 6: e17514.
2. Rolfe DF and Brown GC. Cellular energy utilization and molecular origin of standard metabolic rate in mammals. *Physiol Rev* 1997; 77: 731–758.
3. Fonseca-Azevedo K and Herculano-Houzel S. Metabolic constraint imposes tradeoff between body size and number of brain neurons in human evolution. *Proc Natl Acad Sci USA* 2012; 109: 18571–18576.
4. Mink JW, Blumenschine RJ and Adams DB. Ratio of central nervous system to body metabolism in vertebrates: its constancy and functional basis. *Am J Physiol* 1981; 241: R203–R212.
5. Kennedy C and Sokoloff L. An adaptation of the nitrous oxide method to the study of the cerebral circulation in children; normal values for cerebral blood flow and cerebral metabolic rate in childhood. *J Clin Invest* 1957; 36: 1130–1137.
6. Kuzawa CW, Chugani HT, Grossman LI, et al. Metabolic costs and evolutionary implications of human brain development. *Proc Natl Acad Sci USA* 2014; 111: 13010–13015.
7. Chugani HT. A critical period of brain development: studies of cerebral glucose utilization with PET. *Prev Med* 1998; 27: 184–188.
8. Bianchi S, Stimpson CD, Duka T, et al. Synaptogenesis and development of pyramidal neuron dendritic morphology in the chimpanzee neocortex resembles humans. *Proc Natl Acad Sci USA* 2013; June(110 Suppl 2): 10395–10401.
9. Kuczmarski RJ, Ogden CL, Grummer-Strawn LM, et al. CDC growth charts: United States. *Adv Data* 2000; 8: 1–27.
10. Vandekar SN, Shinohara RT, Raznahan A, et al. Topologically dissociable patterns of development of the human cerebral cortex. *J Neurosci* 2015; 35: 599–609.
11. Sowell ER, Thompson PM, Leonard CM, et al. Longitudinal mapping of cortical thickness and brain growth in normal children. *J Neurosci* 2004; 24: 8223–8231.
12. Beaulieu C. The basis of anisotropic water diffusion in the nervous system - a technical review. *NMR Biomed* 2002; 15: 435–455.
13. Lenroot RK, Gogtay N, Greenstein DK, et al. Sexual dimorphism of brain developmental trajectories during childhood and adolescence. *Neuroimage* 2007; 36: 1065–1073.
14. Feldman HM, Yeatman JD, Lee ES, et al. Diffusion tensor imaging: a review for pediatric researchers and clinicians. *J Dev Behav Pediatr* 2010; 31: 346–356.
15. Nie J, Guo L, Li K, et al. Axonal fiber terminations concentrate on gyri. *Cereb Cortex* 2012; 22: 2831–2839.
16. Taki Y, Thyreau B, Hashizume H, et al. Linear and curvilinear correlations of brain white matter volume, fractional anisotropy, and mean diffusivity with age using voxel-based and region-of-interest analyses in 246 healthy children. *Hum Brain Mapp* 2013; 34: 1842–1856.
17. Blakemore SJ. Imaging brain development: the adolescent brain. Neuroimage. 2012; 61: 397–406.
18. Huttenlocher PR and Dabholkar AS. Regional differences in synaptogenesis in human cerebral cortex. *J Comp Neurol* 1997; 387: 167–178.
19. Lui JC, Garrison P and Baron J. Regulation of body growth. *Curr Opin Pediatr* 2015; 27: 502–510.
20. Durnin J. Basal metabolic rate in man. *Rep Jt FAO/WHO/UNU Expert Consult Energy Protein Requir*, 1981.

21. Satterthwaite TD, Connolly JJ, Ruparel K, et al. The Philadelphia neurodevelopmental cohort: a publicly available resource for the study of normal and abnormal brain development in youth. *Neuroimage* 2016; 124: 1115–1119.

22. Satterthwaite TD, Elliott MA, Ruparel K, et al. Neuroimaging of the Philadelphia neurodevelopmental cohort. *Neuroimage* 2014; 86: 544–553.

23. Satterthwaite TD, Shinohara RT, Wolf DH, et al. Impact of puberty on the evolution of cerebral perfusion during adolescence. *Proc Natl Acad Sci USA* 2014; 111: 8643–8648.

24. Raichle ME and Mintun MA. Brain work and brain imaging. *Annu Rev Neurosci* 2006; 29: 449–476.

25. Huisman MC, van Golen LW, Hoetjes NJ, et al. Cerebral blood flow and glucose metabolism in healthy volunteers measured using a high-resolution PET scanner. *EJNMMI Res* 2012; 2: 63.

26. Barber TW, Brockway JA and Higgins LS. The density of tissues in and about the head. *Acta Neurol Scand* 1970; 46: 85–92.

27. Taki Y, Hashizume H, Sassa Y, et al. Correlation between gray matter density-adjusted brain perfusion and age using brain MR images of 202 healthy children. *Hum Brain Mapp* 2011; 32: 1973–1985.

28. Wu WC, Fernandez-Seara M, Detre JA, et al. A theoretical and experimental investigation of the tagging efficiency of pseudocontinuous arterial spin labeling. *Magn Reson Med* 2007; 58: 1020–1027.

29. Jenkinson M, Beckmann CF, Behrens TE, et al. Fsl. *Neuroimage* 2012; 62: 782–790.

30. Jenkinson M, Bannister P, Brady M, et al. Improved optimization for the robust and accurate linear registration and motion correction of brain images. *Neuroimage* 2002; 17: 825–841.

31. Smith SM. Fast robust automated brain extraction. *Hum Brain Mapp* 2002; 17: 143–155.

32. Smith SM and Brady JM. SUSANa new approach to low level image processing. *Int J Comput Vision* 1997; 23: 45–78.

33. Wang Z, Aguirre GK, Rao H, et al. Empirical optimization of ASL data analysis using an ASL data processing toolbox: ASLtbx. *Magn Reson Imag* 2008; 26: 261–269.

34. Wu WC, Jain V, Li C, et al. In vivo venous blood T1 measurement using inversion recovery true-FISP in children and adults. *Magn Reson Med* 2010; 64: 1140–1147.

35. Jain V, Duda J, Avants B, et al. Longitudinal reproducibility and accuracy of pseudo-continuous arterial spin-labeled perfusion MR imaging in typically developing children. *Radiology* 2012; 263: 527–536.

36. Greve DN and Fischl B. Accurate and robust brain image alignment using boundary-based registration. *Neuroimage* 2009; 48: 63–72.

37. Tustison NJ, Cook PA, Klein A, et al. Large-scale evaluation of ANTs and FreeSurfer cortical thickness measurements. *Neuroimage* 2014; 99: 166–179.

38. Tustison NJ, Avants BB, Cook PA, et al. N4ITK: improved N3 bias correction. *IEEE Trans Med Imag* 2010; 29: 1310–1320.

39. Avants BB, Tustison NJ, Wu J, et al. An open source multivariate framework for n-tissue segmentation with evaluation on public data. *Neuroinformatics* 2011; 9: 381–400.

40. Klein A, Ghosh SS, Avants B, et al. Evaluation of volume-based and surface-based brain image registration methods. *Neuroimage* 2010; 51: 214–220.

41. Avants BB, Tustison NJ, Song G, et al. A reproducible evaluation of ANTs similarity metric performance in brain image registration. *Neuroimage* 2011; 54: 2033–2044.

42. Wang H, Suh JW, Das SR, et al. Multi-atlas segmentation with joint label fusion. *IEEE Trans Pattern Anal Mach Intell* 2013; 35: 611–623.

43. Food and Agriculture Organization of the United Nations., United Nations University. and World Health Organization. In: *Human energy requirements: report of a Joint FAO/WHO/UNU expert consultation*, Rome, 17–24 October 2001. Rome: Food and Agricultural Organization of the United Nations, 2004, p.ix, p.96.

44. Institute of Medicine (U.S.). Panel on Macronutrients. and Institute of Medicine (U.S.). Standing committee on the scientific evaluation of dietary reference intakes. In: *Dietary reference intakes for energy, carbohydrate, fiber, fat, fatty acids, cholesterol, protein, and amino acids*. Washington, D.C.: National Academies Press, 2005, p.xxv, p.1331.

45. R Core Team. *R: A language and environment for statistical computing*. Vienna, Austria: R Core Team: R Foundation for Statistical Computing, 2016.

46. Wood SN. Fast stable restricted maximum likelihood and marginal likelihood estimation of semiparametric generalized linear models. *J R Stat Soc Ser B Stat Methodol* 2011; 73: 3–36.

47. Wood SN. *Generalized additive models: an introduction with R*. Boca Raton, FL: Chapman and Hall/CRC, 2006.

48. Kuczmarski RJ, Ogden CL, Guo SS, et al. 2000 CDC growth charts for the United States: methods and development. *Vital Health Stat 11* 2002; May: 1–190.

49. Harris JJ, Jolivet R and Attwell D. Synaptic energy use and supply. *Neuron* 2012; 75: 762–777.

50. Crone EA and Dahl RE. Understanding adolescence as a period of social-affective engagement and goal flexibility. *Nat Rev Neurosci* 2012; 13: 636–650.

51. Engl E and Attwell D. Non-signalling energy use in the brain. *J Physiol.* 2015; 593: 3417–3429.

52. Raichle ME. Behind the scenes of functional brain imaging: a historical and physiological perspective. *Proc Natl Acad Sci USA* 1998; 95: 765–772.

53. Ginsberg MD, Chang JY, Kelley RE, et al. Increases in both cerebral glucose utilization and blood flow during execution of a somatosensory task. *Ann Neurol* 1988; 23: 152–160.

54. Newberg AB, Wang J, Rao H, et al. Concurrent CBF and CMRGlc changes during human brain activation by combined fMRI-PET scanning. *Neuroimage* 2005; 28: 500–506.

55. Gur RC, Richard J, Calkins ME, et al. Age group and sex differences in performance on a computerized

neurocognitive battery in children age 8-21. *Neuropsychology* 2012; 26: 251–265.

56. Alsop DC, Detre JA, Golay X, et al. Recommended implementation of arterial spin-labeled perfusion MRI for clinical applications: a consensus of the ISMRM perfusion study group and the European consortium for ASL in dementia. *Magn Reson Med* 2015; 73: 102–116.

57. Kubera B, Hubold C, Zug S, et al. The brain's supply and demand in obesity. *Front Neuroenergetics* 2012; 4: 4.

58. Liang J, Matheson BE, Kaye WH, et al. Neurocognitive correlates of obesity and obesity-related behaviors in children and adolescents. *Int J Obes* 2014; 38: 494–506.

59. Willette AA and Kapogiannis D. Does the brain shrink as the waist expands? *Ageing Res Rev* 2015; 20: 86–97.

60. Rosenfield RL, Lipton RB and Drum ML. Thelarche, pubarche, and menarche attainment in children with normal and elevated body mass index. *Pediatrics* 2009; 123: 84–88.

61. Peters A. The selfish brain: competition for energy resources. *Am J Hum Biol* 2011; 23: 29–34.